



Convergent Estimates of Biomass Burning-Derived Atmospheric Ammonia in Peninsular Southeast Asia

Yunhua Chang¹, Yan-Lin Zhang¹, Sawaeng Kawichai², Qian Wang¹, Martin
Van Damme³, Lieven Clarisse³, Tippawan Prapamontol², and Moritz F.
5 Lehmann⁴.

¹Yale-NUIST Center on Atmospheric Environment, Nanjing University of Information Science & Technology,
Nanjing 210044, China

²Research Institute for Health Sciences (RIHES), Chiang Mai University, Chiang Mai 50200, Thailand

³Université libre de Bruxelles (ULB), Spectroscopy, Quantum Chemistry and Atmospheric Remote Sensing
10 (SQUARES), Brussels B-1050, Belgium

⁴Department of Environmental Sciences, University of Basel, Basel 4056, Switzerland

Correspondence to: Yan-Lin Zhang (dryanlinzhang@outlook.com)

Abstract. Ammonia (NH₃) is an important agent involved in atmospheric chemistry and nitrogen cycling. Current
estimates of NH₃ emissions from biomass burning (BB) differ by more than a factor of two, impeding a reliable
15 assessment of their environmental consequences. Combining high-resolution satellite observations of NH₃ columns
with network measurements of the concentration and stable nitrogen isotope composition ($\delta^{15}\text{N}$) of NH₃, we present
coherent estimates on the amount of NH₃ derived from BB in the heartland of Southeast Asia, a tropical monsoon
environment. Our results reveal a strong variability of atmospheric NH₃ levels in time and space across different



landscapes. All evidence in hand suggests that anthropogenic activities are the most important modulating control
20 with regards to the observed patterns of NH_3 distribution in the study area. N-isotope balance considerations
revealed that during the intensive fire period, the atmospheric input from BB accounts for not more than $21 \pm 5\%$
(1σ) of the ambient NH_3 , even at the rural sites and in the proximity of burning areas. Our N-isotope based
assessment of the variation of the relative contribution of BB-derived NH_3 is further validated independently
through the measurements of particulate K^+ , a chemical tracer of BB. Our findings underscore that BB-induced
25 NH_3 emissions in the tropical monsoon environments can be much lower than previously anticipated, with
important implications for future modeling studies to better constrain the climate and air quality effects of wildfires.

1 Introduction

Biomass burning (BB) in tropical vegetation regions due to wildfires has been recognized as a globally important
source of trace gases (including CO_2 , CO, and ozone precursors) and aerosols (mostly black and organic carbon)
30 (Crutzen and Andreae, 1990; Andreae and Merlet, 2001; Shi et al., 2015; Andreae, 2019; Crutzen et al., 1979).
Most BB hotspots occur in West Africa and South America (Crutzen and Andreae, 1990; van der Werf et al., 2006;
Shi et al., 2015), but recent studies have highlighted the importance also of Southeast (SE) Asia in this regard,
mainly because of the much higher population densities near intensive fire burning areas (Huang et al., 2013;
Marlier et al., 2013; Lee et al., 2017; Betha et al., 2014). The climate over large parts of SE Asia is governed by a
35 wet (typically May, June, July) and dry (typically February, March, April) season caused by seasonal shifts in the
monsoon winds. During the dry season, dry plant materials (e.g., forest, peatland, banana leaf) readily ignite,
resulting in large wildfires that can markedly modify the atmospheric composition in the tropics, while the tropical
rain belt causes plentiful rainfall during summer, preventing such fires during the rainy season (Lee et al., 2017;
Chu et al., 2018).



40 Besides carbon soot, BB also emits large amounts of reactive nitrogen compounds (Lobert et al., 1990; Bauters et al., 2018), in particular ammonia (NH_3), which is believed to represent the major source of NH_3 during intensive fires period (Akagi et al., 2011; Whitburn et al., 2015). However, these emissions are subject to large uncertainties (differences by a factor of two or greater). (Bray et al., 2018; Whitburn et al., 2015; Whitburn et al., 2016b; Van Damme et al., 2015b) For example, BB is probably the second most important NH_3 source after agriculture, 45 contributing 11-23% of the global burden (Paulot et al., 2017; Bouwman et al., 1997). Minor NH_3 sources include fossil fuel burning and biogenic activity (Chang et al., 2012; Chang et al., 2016b; Chang et al., 2019b; Chang et al., 2020). A recent paper also highlighted the underestimated importance of industrial emissions (Van Damme et al., 2018). Once emitted in the atmosphere, NH_3 is rapidly removed by dry or wet deposition (Asman et al., 1998). Excess NH_3 is known to be responsible for several environmental issues: eutrophication of terrestrial and aquatic 50 ecosystem, soil acidification, and loss of plant diversity (Sutton et al., 2008; Aneja et al., 2008; Sutton et al., 2011). In the atmosphere, NH_3 can neutralize acid gases (mostly sulfuric acid, nitric acid or hydrochloric acid), resulting in the formation of secondary aerosols that in turn negatively affect climate and human health (Wang et al., 2011; Wang et al., 2013; Paulot and Jacob, 2014; Souri et al., 2017).

To assess the environmental impacts of BB (e.g., air quality and climate change), atmospheric chemistry models 55 incorporating BB-related emissions have widely been used over the past decades (Huang et al., 2013; Aouizerats et al., 2015; Wang et al., 2013; Wang et al., 2011; Souri et al., 2017) but are afflicted with a relatively large uncertainty regarding the input parameters used in the models (Hantson et al., 2016; Whitburn et al., 2015; Paulot et al., 2017). The uncertainties, for example, for carbon emissions and for other trace gases (including NH_3), can be over 200% (Whitburn et al., 2015; Paulot et al., 2017; Zhu et al., 2013; Pan et al., 2019). In recent years, 60 hyperspectral sounders on board satellites have demonstrated their capabilities to directly measure tropospheric column concentrations of NH_3 gas (Van Damme et al., 2018; Van Damme et al., 2014; Van Damme et al., 2015b; Clarisse et al., 2009). Satellite observations therefore offer a “top-down” alternative to the bottom-up estimates.



Still, the biggest challenge of satellite-based NH_3 assessments is the requirement for the atmosphere to be cloud-free during observations, and the need for a sizeable temperature difference between land or sea surface and the atmosphere (Van Damme et al., 2015a; Whitburn et al., 2015; Martin, 2008; Streets et al., 2013; Clarisse et al., 2010).

Large uncertainties remain regarding global or regional atmospheric budgets of NH_3 , and the attribution of emissions to specific sources, emphasizing the need for independent verification methods. An impressive body of previous work has studied the BB influence on the concentration and composition of aerosols in SE Asia (Betha et al., 2014; Aouizerats et al., 2015; Lee et al., 2017; Bikkina et al., 2019). However, to our knowledge, there are no reports on the detailed spatiotemporal patterns of atmospheric NH_3 concentration and nitrogen isotopic composition ($\delta^{15}\text{N-NH}_3$) associated with BB in this region. Due to isotopic fractionation associated with NH_3 production, pyrogenic NH_3 displays a distinctly higher $\delta^{15}\text{N-NH}_3$ ($\delta^{15}\text{N}$ defined as $(R_{\text{sample}}/R_{\text{standard}} - 1) \times 1000$, where R refers to the $^{15}\text{N}/^{14}\text{N}$ ratio in a sample or a standard) than temperature-dependent volatilized sources (Felix et al., 2013; Chang et al., 2016a). The N isotopic analysis of ambient NH_3 has been proven a useful tool to constrain sources of NH_3 emissions in the atmosphere, where both natural and anthropogenic activities are relevant (Chang et al., 2019b; Chang et al., 2019a; Elliott et al., 2019). Here, we integrate high-resolution satellite observations with discrete NH_3 concentration measurements and $\delta^{15}\text{N-NH}_3$ data obtained from a regional passive monitoring network during and after the dry season of large-scale forest fires in the mountain areas of northern Thailand, SE Asia.

2 Methods

2.1 Site description

Surrounded by the mountain ranges of the northern Thailand highlands, the Chiang Mai Province covers an area of approximately 20107 km², with a total population of over 1.7 million. Chiang Mai is characterized by a tropical



monsoon climate, tempered by the low latitude and moderate elevation, with warm to hot weather year-round.
85 Some 70% of the area is covered by forests, and 13.4% of the area is under agriculture. A continuing environmental
issue in Chiang Mai is the smoke pollution from wildfires that primarily occurs every year towards the end of the
dry season between February and April (Tsai et al., 2013) before the relatively cool and rainy season from May on.
During the period from March to July 2018, ambient NH_3 concentrations and $\delta^{15}\text{N-NH}_3$ values were determined at
90 different land use regimes indicated), while Fig. S1 reports meteorological data for Chiang Mai and Table S1 details
the information of each station.

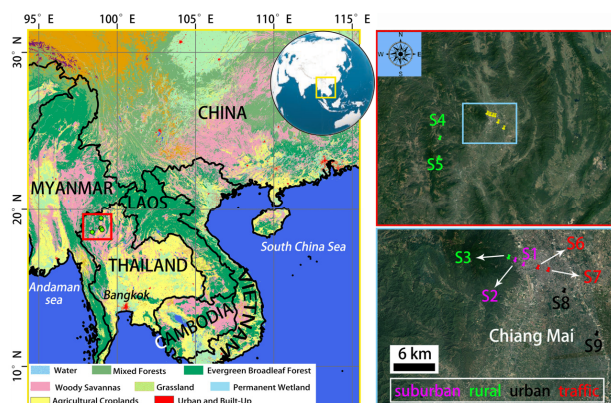


Figure 1. Location of sampling sites. Land-cover map (left; revised from Chang et al.,) with zoom-in in lower
panels (right). The chosen sampling sites are representative for gradient in land use from urban to rural. Images in
95 the right are obtained from © Google Maps.



2.2 Sampling and laboratory analysis

In order to obtain information regarding the spatial and temporal variability of NH_3 concentrations over Chiang Mai, ambient gas-phase NH_3 concentrations at each site were collected weekly using passive sampling devices (PSD) (ALPHA - Adapted Low-cost, Passive High Absorption; Centre for Ecology and Hydrology, Edinburg, UK) (Chang et al., 2016a). The ALPHA PSD is a circular polyethylene vial (26 mm height, 27 mm diameter) with one open end. The vial holds a 25 mm phosphorous acid-impregnated filter and a PTFE membrane for gaseous NH_3 diffusion. These PSDs have been widely used in Europe, China, and the US, and are capable of detecting NH_3 concentrations as low as $0.03 \mu\text{g m}^{-3}$ (Chang et al., 2016a; Puchalski et al., 2011; Liu et al., 2013; Tang et al., 2018). In the laboratory, the ALPHA filter samples were soaked in 10 mL deionized water ($18 \text{ M}\Omega\cdot\text{cm}$) in a 15 mL vial for 30 min with occasional shaking. Concentrations of NH_3 -derived NH_4^+ in extracts were determined using a DionexTM ICS-5000⁺ system (Thermo Fisher Scientific, Sunnyvale, USA). The IC system was equipped with an automated sampler (AS-DV), an IonPac CG12A guard column, and a CS12A separation column. Aqueous methanesulfonic acid (MSA, 30 mM L^{-1}) served as eluent at a flow rate of 1 mL min^{-1} . The isotopic analysis of the extracted NH_4^+ was based on the isotopic analysis of nitrous oxides (N_2O) after chemical conversion (Liu et al., 2014). More precisely, dissolved NH_4^+ in DI extracts was oxidized to NO_2^- by alkaline hypobromite (BrO^-), and then reduced to N_2O by hydroxylamine hydrochloride ($\text{NH}_2\text{OH}\cdot\text{HCl}$). The produced N_2O was analyzed using a purge and cryogenic trap system (Gilson GX-271, IsoPrime Ltd., Cheadle Hulme, UK), coupled to an isotope ratio mass spectrometer (PT-IRMS) (IsoPrime 100, IsoPrime Ltd., Cheadle Hulme, UK) (Liu et al., 2014). In order to correct for any machine drift and procedural blank contribution, international NH_4^+ (IAEA N1, USGS 25, and USGS 26) standards were processed in the same way as samples (Liu et al., 2014). The analytical precision for N isotope analyses was better than 0.5%.



2.3 Isotope-based source apportionment

Isotopic mixing models represent valuable tools to estimate the fractional contributions of multiple sources (emission sources of NH_3 in this study) within a mixture (the ambient NH_3 in this study) (Layman et al., 2012). By explicitly taking into account the uncertainties associated with the isotopic signatures of single sources and the N isotope fractionation during transformations, the application of Bayesian methods to stable isotope mixing models yields robust probability estimates on source apportionments, and its application to natural systems is more appropriate than the application of simple linear mixing models (Parnell et al., 2010). Here, a novel Bayesian approach using a mixing model, implemented in the software package SIAR (Stable Isotope Analysis in R), was used to resolve multiple NH_3 source categories by generating potential solutions of source apportionment as true probability distributions of the single source contribution to the total NH_3 pool. The generation of such source contribution probability distributions allows estimating likelihood ranges of source contributions even at under-constrained conditions (i.e., the number of potential sources exceeds the number of different isotope system parameters + 1). The SIAR package is available to download from the packages section of the Comprehensive R Archive Network site (CRAN; <http://cran.r-project.org/>), which has been widely applied in a number of fields (Chang et al., 2019a; Chang et al., 2019b). Model frame and computing methods are detailed in Text S1.

2.4 Satellite observations of ammonia and fires

NH_3 total columns (molec cm^{-2}) are retrieved from the Infrared Atmospheric Sounding Interferometer (IASI) observations. IASI instruments are onboard the Metop satellite series; in this work, we use IASI/Metop-A (launched in 2006) and IASI/Metop-B (launched in 2012) data. Both instruments have an overpass time around 9:30 am and pm (local solar time when crossing the equator) and therefore provide in total a global coverage four times a day. The retrieval strategy, based on artificial neural networks, is fully detailed in previous work (Whitburn et al., 2016a; Van Damme et al., 2017). Here we only consider morning observations, as they are more sensitive to the lower

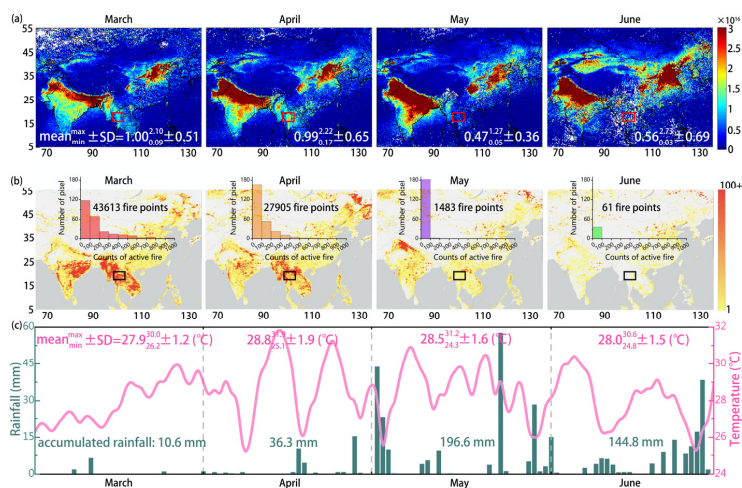


layer of the atmosphere. Fire Radiative Power (FRP) from the Moderate Resolution Imaging Spectroradiometer
140 (MODIS) and fire counts derived from the 375-m Visible Infrared Imaging Radiometer Suite (VIIRS) are also used
(Li et al., 2020).

3 Results and discussion

3.1 Satellite-observed NH₃ distributions probably linked with biomass burning

Figure 2a illustrates the monthly spatial distribution of NH₃ columns obtained from IASI in 2018 at a spatial
145 resolution of 0.25° × 0.5° cells. Our study area is set within a large domain of 5.00° × 3.25° (red and black rectangles
in Fig. 2a and Fig. 2b, respectively), in which totally 260 gridded pixels (0.25° × 0.25° per cell) are used for dividing
active fire points (Fig. 2b). Intriguingly, from this plot, one is tempted to conclude that fires do play a very important
role in NH₃ emissions, as the NH₃ columns are much higher in March and April (dry season), which is coincident
with high number of monthly fire activities (indicated by the number of fire points). Further, using 11 years (2008-
150 2018) of IASI satellite data, Figure S2 presents a climatology of monthly NH₃ columns over Chiang Mai at a much
finer spatial resolution, which also support the pervasive contribution of BB during dry season (March and April).
Based on the average observed temporal distribution of satellite-constrained wildfires, the sampling period in this
study can be divided into two contrasting fire-regime periods, i.e., BB season (March and April) and non-BB season
(May and June). Interestingly, however, although the number of fire points in March (43613 points) is significantly
155 (p < 0.01) higher than that in April (27905 points) (Fig. 2b), the average NH₃ column in March is nearly the same
as that in April (Fig. 2a). This implies that there is not a one-to-one relationship between BB and NH₃ emissions,
and in turn that other sources or factors (e.g., soil dryness, agricultural emissions, precipitation, temperature
dependence, etc.) must also play a significant role.



160 Figure 2. (a) Monthly (March, April, May, June) spatial distributions of the NH₃ total columns (molecules cm⁻²) in
 2018 obtained from the satellite measurements by the Infrared Atmospheric Sounding Interferometer
 (IASI)/MetOp-A instrument in 0.25° × 0.5° cells. (b) Monthly distributions of gridded counts of active fire pixels
 (0.25° × 0.25° per cell) derived from the 375-m Visible Infrared Imaging Radiometer Suite (VIIRS). The red and
 black squares indicate our study area in Chiang Mai. (c) Daily variations of (°C) and rainfall (mm) in Chiang Mai
 165 City.

Given that the average monthly temperature varies only little, in contrast to the drastic change of rainfall during
 our study period (Fig. 2c), it is reasonable to assume that temperature-dependent NH₃ volatilization is not the main
 driver of changes in the NH₃ columns. The amount of rainfall, on the other hand, can have multi-faceted impact on
 NH₃ emissions. First of all, there is an obvious link between precipitation rates and the number of wildfires, and, if
 170 BB is a major NH₃ emission source, we can also expect a relationship between the NH₃ columns and monthly
 rainfall rates. Secondly, and maybe more importantly, rain will dissolve atmospheric particulate NH₄⁺, and will act
 to clean the air from NH₃, which may partly explain the low NH₃ levels during May and June. On the other hand,



comparison between March and April reveals higher NH_3 levels in April despite higher rain rates, suggesting that other processes than BB and rain-scavenging of BB-derived NH_3 must be relevant factors. In Fig. 3a and 3b, we
175 superimposed the orography at the scale of the study area (Chiang Mai and surrounding mountains) onto the images of year-long averaged MODIS FRP (Fire Radiative Power) and IASI- NH_3 for 2018, respectively. Just by visual evaluation it seems obvious that there is no strong correlation between fire intensity/number of fires and the observed IASI- NH_3 , suggesting only limited influence of BB on NH_3 . Yet more strikingly, the IASI- NH_3 distribution matches that of the population density quite well (Fig. 3c). More precisely, hot spots of atmospheric
180 NH_3 (Fig. 3b) appear to be concentrated in urban areas with dense population. Hence, our satellite remote sensing observations suggest a significant influence of non-BB emissions on NH_3 concentrations, seemingly related to urban anthropogenic activities.

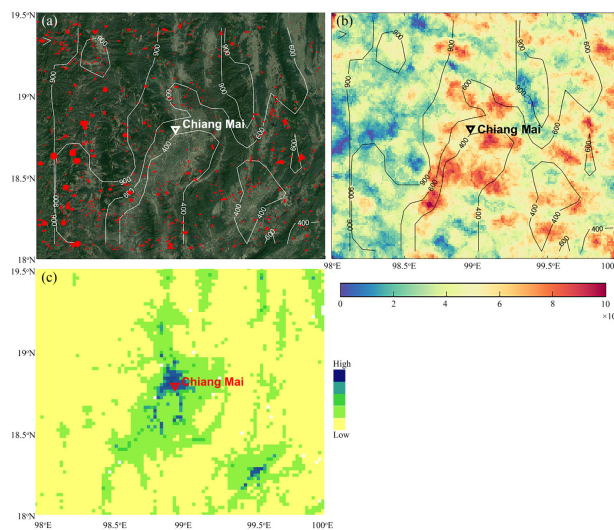




Figure 3. (a) The MODIS FRP (fire radiative power) (the size of red dots is proportional to FRP value) and (b) the
185 IASI Metop-A and Metop-B averaged NH_3 distribution (molec cm^{-2}) for 2018. (c) Number of people per grid-cell
in the Chiang Mai area in 2018 at a resolution of 3 arc minute.

3.2 Discrete concentration measurements confirm urban areas as hot spots of NH_3 emissions

A total of 153 passive samples were collected in this study for analyzing NH_3 concentrations and reported in Fig.
4. Considering all weekly samples, the range of atmospheric NH_3 concentrations over Chiang Mai was from 2.5 to
190 $46.4 \mu\text{g m}^{-3}$, with a mean ($\pm 1\sigma$) and median value of $14.5 (\pm 9.2)$ and $11.4 \mu\text{g m}^{-3}$, respectively. Consistent with
the IASI satellite-based NH_3 assessment, the weighted average NH_3 concentration ($\text{mean}_{\text{min}}^{\text{max}} \pm 1\sigma$) was
significantly ($p < 0.01$) higher during the dry season when there were significantly ($p < 0.01$) more wild fires
($20.6_{6.8}^{46.4} \pm 9.8 \mu\text{g m}^{-3}$) than that during the rainy season ($10.2_{2.5}^{31.9} \pm 5.7 \mu\text{g m}^{-3}$). Again, it is tempting to
conclude that there is a direct link between higher atmospheric NH_3 levels and the higher number of BB events.
195 However, there are several aspects that appear to preclude BB at least as the main or only driver of ambient NH_3
concentrations. Firstly, from a global perspective, the ambient NH_3 concentrations we measured in northern
Thailand are generally lower than in tropical regions with dense population or intensive agricultural production
(also see Fig. 2a) (Carmichael et al., 2003; Chang et al., 2016b). Secondly, within the study area, large spatial
differences in NH_3 concentrations were found (Fig. 4). Yet, despite their proximity to wildfires at the time, the
200 three rural sites always displayed the lowest NH_3 concentrations ($8.3_{2.5}^{26.8} \pm 4.6 \mu\text{g m}^{-3}$; Fig. 4; see detailed
discussion in the next section).

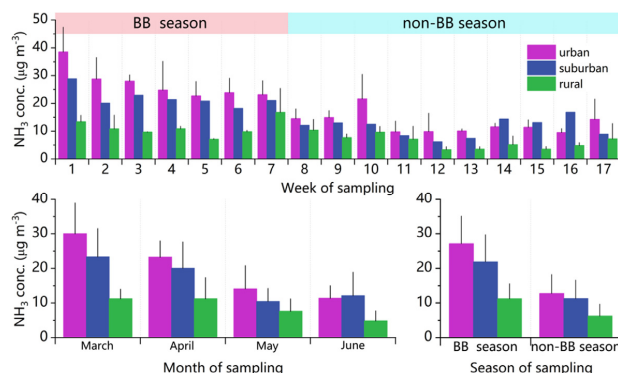


Figure 4. Temporal variations of measured NH_3 concentrations ($\mu\text{g m}^{-3}$) between sites of different land-use regimes. The error bar indicates one standard deviation.

205 Although afflicted with large uncertainties, it is well accepted that, globally, atmospheric NH_3 is primarily emitted by agricultural activities and biomass burning (Asman et al., 1998; Bouwman et al., 1997). One could expect the NH_3 concentrations in the atmosphere over rural environments with lush vegetation and agricultural land-use to be higher than those in (sub)urban areas, where agricultural activities are mostly absent. In our study, the average NH_3 concentrations at the nine sites are $19.5_{6.5}^{39.4} \pm 9.5$ (S1; suburban), $11.9_{4.5}^{19.7} \pm 4.6$ (S2; suburban), $8.8_{4.4}^{16.6} \pm 3.9$ (S3; rural), $9.0_{2.8}^{26.8} \pm 5.8$ (S4; rural), $7.0_{2.5}^{13.7} \pm 3.8$ (S5; rural), $20.2_{9.1}^{40.5} \pm 8.6$ (S6; urban traffic), $18.1_{7.2}^{46.1} \pm 12.1$ (S7; urban traffic), $19.6_{4.2}^{46.4} \pm 10.1$ (S8; urban), and $16.6_{6.7}^{30.6} \pm 8.0$ (S9; urban) $\mu\text{g m}^{-3}$ (see also compilation in Fig. 4). Thus, against current paradigms, the NH_3 concentrations, from high to low, display clearly an urban ($18.6_{4.2}^{46.4} \pm 9.7$, $n = 68$) to suburban ($15.6_{4.5}^{39.4} \pm 8.3$, $n = 34$) to rural ($8.3_{2.5}^{26.8} \pm 4.6$, $n = 51$) gradient. Such gradient can be taken as evidence that non-agricultural activities (including on-road traffic), at least in some

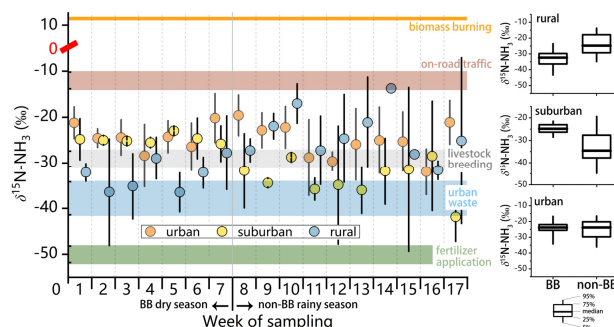
215 regions, can overtake agriculture and/or BB as the dominant NH_3 source in urban areas.



Indeed, a growing body of studies confirm that the urban atmosphere can be a hot spot of NH_3 release. Non-agricultural activities like wastewater treatment, coal combustion, solid garbage, vehicular exhaust, and urban green space also contribute to NH_3 emissions (Chang et al., 2016a; Chang et al., 2019b; Teng et al., 2017; Chang et al., 2015; Li et al., 2016; Sun et al., 2017). For example, high vehicular NH_3 emissions from noble metal-based three-way catalysts (TWCs) have been demonstrated in chassis dynamometer vehicle experiments, road tunnel tests, and through ambient air measurements (Huang et al., 2018; Chang et al., 2016b; Chang et al., 2019b).

3.3 N isotopic constraints on the sources of natural and anthropogenic NH_3

The correlative analysis of spatiotemporal concentration patterns with variations in land use effects provides first qualitative constraints with regards to the relative importance of natural/BB and anthropogenic NH_3 emissions, but it is insufficient when a more quantitative assessment is required. The N-isotopic composition of NH_3 (i.e., $\delta^{15}\text{N-NH}_3$) can provide help in this regard, as it is sensitive to changes of NH_3 sources with distinct isotopic composition (Elliott et al., 2019; Felix et al., 2013). $\delta^{15}\text{N-NH}_3$ values determined in this study ($-27.04_{-46.28}^{-12.35} \pm 7.22\%$, $n = 145$) show a relatively large variability in time and space (Fig. 5). NH_3 emitted from the five major NH_3 sources displays distinct isotopic signatures (N-fertilizer application, $-50.0 \pm 1.8\%$; urban waste volatilized sources, $-37.8 \pm 3.6\%$; livestock breeding, $-29.1 \pm 1.7\%$; on-road traffic, $-12.0 \pm 1.8\%$; biomass burning, 12%) (see colored bars in Fig. 4) (Chang et al., 2016a; Kawashima and Kurahashi, 2011; Chang and Ma, 2016). Thus, the measurement of $\delta^{15}\text{N-NH}_3$ can be used to distinguish between specific sources, and to quantify their contribution to the measured total NH_3 pool. As a first step, we examine the spatiotemporal characteristics of the measured $\delta^{15}\text{N-NH}_3$ relative to the N isotopic source signatures to infer seasonal changes of NH_3 sources.



235

Figure 5. (left) Weekly-based variations of the $\delta^{15}\text{N}$ values (‰) of ambient NH_3 measured in urban, suburban, and rural environments (setting 0 as the breaking point). The error bars indicate two standard deviations. (right) Box plots of the distribution of $\delta^{15}\text{N}$ - NH_3 during BB season and non-BB season for each type of sampling sites.

The lowest $\delta^{15}\text{N}$ - NH_3 values were observed at the rural sites (S3-S5) during the dry season
 240 $(-32.72_{-20.38}^{-46.28} \pm 6.46\text{‰}, n = 21)$. These $\delta^{15}\text{N}$ values are much lower than the $\delta^{15}\text{N}$ of BB-related NH_3 and indicate the pervasive influence of agricultural NH_3 emissions in rural environments, rather than BB. During the rainy season, a drastic increase of $\delta^{15}\text{N}$ - NH_3 $(-23.97_{-37.99}^{-12.35} \pm 7.50\text{‰}, n = 22)$ at the rural sites was observed. Again, if BB was the dominating modulator of NH_3 levels, an increased contribution from of BB-derived NH_3 during the dry versus the wet season in rural areas should have resulted in higher, and not lower $\delta^{15}\text{N}$ - NH_3 values. The
 245 increased $\delta^{15}\text{N}$ - NH_3 during the non-BB (i.e., rainy) period can probably be explained by the fact that agricultural NH_3 emissions with low $\delta^{15}\text{N}$ - NH_3 can be dramatically lowered by continuous and heavy rainfall (Zheng et al., 2018; Chang et al., 2019a) so that at low levels, local sources can become more important (e.g., residential kitchens, nearby burning of biofuels for cooking).



As for the urban sites, the mean $\delta^{15}\text{N-NH}_3$ values at S6, S7, S8, and S9 were $-23.95_{-34.00}^{-16.35} \pm 4.61\%$,
250 $-25.53_{-35.01}^{-14.10} \pm 6.11\%$, $-24.47_{-33.08}^{-16.86} \pm 4.20\%$, and $-25.32_{-39.44}^{-17.13} \pm 7.75\%$, respectively. The overall
average $\delta^{15}\text{N-NH}_3$ value at the four urban sites ($-24.82_{-39.44}^{-14.10} \pm 5.74\%$, $n = 68$) was significantly ($p < 0.01$) higher
than that at the rural ($-28.24_{-46.28}^{-12.35} \pm 8.22\%$, $n = 43$) and suburban ($-29.94_{-45.62}^{-18.78} \pm 7.35\%$, $n = 34$) sites,
respectively, indicating a greater contribution of NH_3 emissions from pyrogenic (e.g., on road traffic) sources. The
average value of urban $\delta^{15}\text{N-NH}_3$ during the dry season ($-24.21_{-34.47}^{-14.10} \pm 4.82\%$, $n = 28$) was very similar to the
255 average value observed during the rainy season ($-25.25_{-39.44}^{-15.31} \pm 6.33\%$, $n = 40$), after the pronounced decrease
of NH_3 concentrations due to wet removal. This rather minor difference can hardly be ascribed to the influence of
BB emissions, given the large seasonal fluctuation of wildfire intensity mentioned above. Based on the absolute
 $\delta^{15}\text{N-NH}_3$ values in the urban settings, and their rather invariant temporal trends, we argue that vehicle/transport-
related is a more important and apparently steady source of pyrogenic NH_3 in the studied urban areas.

260 The two suburban sites (S1 and S2) are located geographically within the transition zone between the urban and
rural environments, and this transitional character seems also indicated by their intermediate $\delta^{15}\text{N-NH}_3$ values
($-29.94_{-45.62}^{-18.78} \pm 7.35\%$, $n = 34$). However, interestingly, in comparison to the urban and rural sites, the overall
 $\delta^{15}\text{N-NH}_3$ value for the two suburban sites was significantly ($p < 0.01$) higher during the BB season
($-24.84_{-28.56}^{-21.49} \pm 2.29\%$, $n = 14$) than that during non-BB season ($-33.52_{-45.62}^{-18.78} \pm 7.59\%$, $n = 20$) (Fig. 5). In
265 fact, among the three different land-use regimes, during the BB season, the average $\delta^{15}\text{N-NH}_3$ was highest for the
suburban sites, and closer the NH_3 isotopic signatures of pyrogenic sources, raising questions as to how important
the contribution of BB versus road traffic in the suburban areas during BB season really is.



3.4 Isotope-based quantification of BB contribution to ambient NH₃

There are several challenges that need to be overcome when trying to more accurately quantify the contribution of BB emissions to ambient NH₃ based on N isotope data. Firstly, given the use of only one isotope parameter ($\delta^{15}\text{N}$; in contrast to NO_x where also the $\delta^{18}\text{O}$ can be analyzed), more than three potential NH₃ sources (e.g., urban and suburban sites) will introduce large uncertainties in isotopic endmember mixing models in terms of quantifying their relative contributions to the ambient NH₃ (Chang et al., 2015). Secondly, atmospheric wet scavenging could further compromise/alter the primary NH₃ N isotopic signatures (Elliott et al., 2019; Zheng et al., 2018; Chang et al., 2019a). For these reasons, we focus here on the samples collected at the three rural sites during the dry BB season (lasting seven weeks) to isotopically examine the contribution of BB emissions to ambient NH₃. We separated these samples into seven groups based on the week of their sampling, and we integrated the measured $\delta^{15}\text{N-NH}_3$ values as well as the N isotopic signatures of potential NH₃ sources (i.e., biomass burning, livestock breeding, fertilizer application) into the Bayesian isotopic mixing model (see Text S1 for details). The results of NH₃ source apportionment are reported in Fig. 6. With a certain degree of variability, the contribution of BB to the ambient NH₃ in the rural areas during the seven weeks of sampling in the dry season was only 21.0% ($\pm 4.7\%$). Hence, NH₃ emission from BB significantly less important than from livestock breeding ($37.1 \pm 7.1\%$) and fertilizer application ($41.8 \pm 5.9\%$). This comes at a surprise, given the fact that the study area belongs to one of the most important BB regions in SE Asia, or even in the world, and the samples used for isotopic source apportionment were collected during the season of intensive BB.

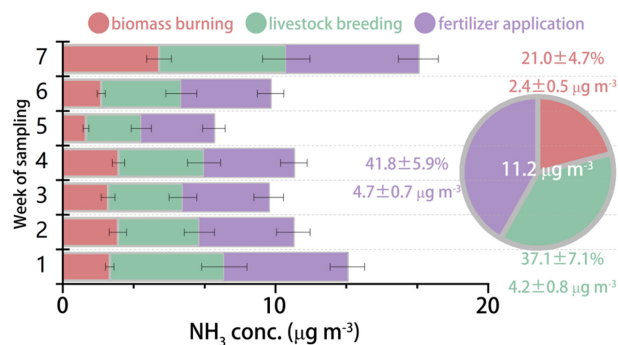


Figure 6. Source apportionment results of ambient NH_3 in rural areas during the dry season based on Bayesian isotopic mixing modelling and the isotopic source signatures. The error bars indicate two standard deviations.

During the dry season, we also analyzed particulate potassium (K^+), a chemical tracer of biomass combustion, at two rural sites (S4, S5; in 39 daily fine-particle ($\text{PM}_{2.5}$) samples). The particulate K^+ data offer a valuable opportunity to validate our isotope-based source apportionment results. Again, we divided the dry-season data set into seven groups based on the week of NH_3 passive sampling. The correlation between the particulate K^+ concentration and the total NH_3 concentration at the rural sites was rather poor ($r^2 = 0.43$; blue symbols in Fig. 7a). Such a weak correlation supports our conclusion regarding the isotope-based source apportionment results (see above), providing additional independent evidence that BB can hardly be the dominant source of NH_3 during the sampling period at the studied rural areas. In contrast, the correlation between the particulate K^+ concentration and the estimated BB-derived NH_3 concentration (instead of total NH_3) is much better ($r^2 = 0.76$; Fig. 7a), and thus further validates our modeling approach. While the independent particulate K^+ data further increase our confidence in the N-isotope based assessment, still some uncertainty remains with regards to the robustness of the endmember source $\delta^{15}\text{N}$ values, potential source-altering effects, and in turn our estimates on the BB-associated NH_3 contribution. In other words, the latter is probably sensitive to the considered range in the $\delta^{15}\text{N}$ of potential NH_3



emission sources, and this range may be quite large/uncertain at least for some of the sources. The $\delta^{15}\text{N-NH}_3$ from BB, in particular, is only poorly constrained, with hardly any reports from the literature (e.g., (Kawashima and Kurahashi, 2011)). In recent chamber experiments, we found that the $\delta^{15}\text{N-NH}_3$ produced by combustion of a
305 variety of biomass types (subtropical trees and agricultural residues) ranged between -11.8‰ and -4.6‰ (Chang et al., 2016, 2019a), which is distinctly lower than the N isotopic signature of BB-emitted NH_3 (12‰) determined previously (Kawashima and Kurahashi, 2011), and adopted in this study. Assuming that the true N isotopic signatures of BB-emitted NH_3 in the study area falls somewhere within the range of -12‰ and 12‰ (based on our published data (Chang et al., 2016,2019a) and the value reported in (Kawashima and Kurahashi, 2011)), we re-
310 calculated the source apportionment estimates as function of the different $\delta^{15}\text{N}$ values for BB-emitted NH_3 (Fig. 7b). The estimates are not sensitive to the choice of the N isotopic composition of the BB-associated NH_3 source. Specifically, independent of the chosen $\delta^{15}\text{N-NH}_3$ value, BB is always the least important of the three main NH_3 sources in rural areas, contributing not more than 29.6%. This is because that although the isotopic signatures of BB-emitted NH_3 have a wide range of $\delta^{15}\text{N}$ values, their $\delta^{15}\text{N-NH}_3$ values are still significantly ($p < 0.01$) higher
315 (i.e., without overlap as shown in Fig. 4) than the measured $\delta^{15}\text{N}$ values of ambient NH_3 at the rural sites.

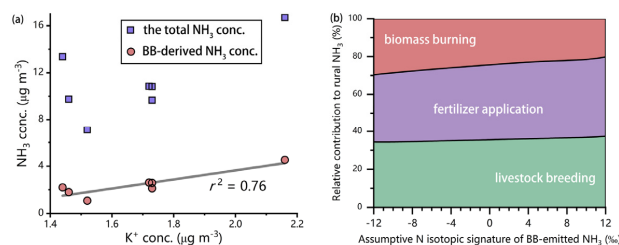


Figure 7. (a) Scatter plots of the aerosol K⁺ concentrations versus total NH₃ concentrations, as well as the NH₃ concentrations from BB emissions, at the rural sites during the dry season. (b) Bayesian isotope modelling-based



source apportionment results of ambient NH_3 at the rural sites during dry season, as function of the assumed N
320 isotopic signatures of BB-emitted NH_3 .

As illustrated by the pie chart in Fig. 6, the average contribution of BB to ambient NH_3 at the rural sites during the
season of intensive fire events is $2.4 \mu\text{g m}^{-3}$, which can be regarded as the maximum possible concentration of BB-
emitted NH_3 for the urban and rural sites, which are much further away from the fire areas. Based on the total NH_3
concentrations measured at the other sites, we calculate, in turn, that the contribution of BB to the ambient NH_3 in
325 the urban and suburban areas are on the order of 9.6% (ranging from 5.2% to 14.8%) and 12.3% (ranging from 6.1%
to 19.9%), respectively.

4 Conclusion

In this study, we integrated satellite constraints on atmospheric NH_3 levels and fire intensity, discrete NH_3
concentration measurement, and N isotopic analysis of NH_3 in order to assess the regional-scale contribution of
330 BB to ambient NH_3 in the heartland of Southeast Asia. The combined approach provides a cross-validation
framework for source apportioning of NH_3 in the lower atmosphere and will thus help to ameliorate predictions of
BB emissions beyond the tropics, particularly in areas of high vegetation fire risk. Our results suggest that during
the dry wildfire season, BB emissions represent a ubiquitous but comparatively small NH_3 source, which accounts
for 9.6%, 12.3%, and 21.0% of ambient NH_3 in urban, suburban, and rural environments, respectively. While we
335 do not claim that our results necessarily apply also at the global scale, and we do not question that globally BB is
one of the most important NH_3 sources, we find that at least in the heartland of SE Asia, BB related NH_3 emissions
to the atmosphere are rather moderate, and vary significantly in time and space. Both satellite observations and
field/ground-based measurements capture these variations. Our findings underscore that BB-induced NH_3
emissions in tropical monsoon environments can be much lower than previously anticipated. Existing atmospheric
340 transport models may overestimate current, and likely future, NH_3 emissions under changing climate conditions.



While the full implications of our results remain to be explored, they promise to provide important guidance for revising NH₃ emissions from BB in atmospheric transport models to assess on air quality, human health and climate change.

Acknowledgements

345 This study was supported by the International (regional) Cooperation and Exchange Project (NSFC-TRF project; Grant no. 41761144056), the National Natural Science Foundation of China (Grant nos. 41975166, 41977305, 41761144056, 41705100), the Provincial Natural Science Foundation of Jiangsu (Grant no. BK20180040, BK20170946), the special fund of State Key Joint Laboratory of Environment Simulation and Pollution Control (Grant no. 19K01ESPCT). Lieven Clarisse and Martin Van Damme are respectively a research associate and a
350 postdoctoral researcher supported by the F.R.S.-FNRS.

Conflict of interest

The authors declare that they have no competing interests.

Data availability statement

Time series of data used in this paper can be found online (at <https://doi.org/10.5281/zenodo.4025673>).

355 References

- Akagi, S. K., Yokelson, R. J., Wiedinmyer, C., Alvarado, M. J., Reid, J. S., Karl, T., Crounse, J. D., and Wennberg, P. O.: Emission factors for open and domestic biomass burning for use in atmospheric models, *Atmos. Chem. Phys.*, 11, 4039-4072, 10.5194/acp-11-4039-2011, 2011.
- 360 Andreae, M. O., and Merlet, P.: Emission of trace gases and aerosols from biomass burning, *Global Biogeochem Cy*, 15, 955-966, 10.1029/2000gb001382, 2001.
- Andreae, M. O.: Emission of trace gases and aerosols from biomass burning – an updated assessment, *Atmos. Chem. Phys.*, 19, 8523-8546, 10.5194/acp-19-8523-2019, 2019.



- Aneja, V. P., Schlesinger, W. H., and Erisman, J. W.: Farming pollution, *Nat Geosci*, 1, 409-411, Doi 10.1038/Ngeo236, 2008.
- 365 Aouizerats, B., van der Werf, G. R., Balasubramanian, R., and Betha, R.: Importance of transboundary transport of biomass burning emissions to regional air quality in Southeast Asia during a high fire event, *Atmos. Chem. Phys.*, 15, 363-373, 10.5194/acp-15-363-2015, 2015.
- Asman, W. A., Sutton, M. A., and Schjørring, J. K.: Ammonia: emission, atmospheric transport and deposition, *New Phytol*, 139, 27-48, 1998.
- 370 Bauters, M., Drake, T. W., Verbeeck, H., Bodé, S., Hervé-Fernández, P., Zito, P., Podgorski, D. C., Boyemba, F., Makelele, I., Cizungu Ntaboba, L., Spencer, R. G. M., and Boeckx, P.: High fire-derived nitrogen deposition on central African forests, *Proceedings of the National Academy of Sciences*, 115, 549-554, 10.1073/pnas.1714597115, 2018.
- Betha, R., Behera, S. N., and Balasubramanian, R.: 2013 Southeast Asian Smoke Haze: Fractionation of Particulate-Bound Elements and Associated Health Risk, *Environmental Science & Technology*, 48, 4327-4335, 10.1021/es405533d, 2014.
- Bikkina, S., Haque, M. M., Sarin, M., and Kawamura, K.: Tracing the Relative Significance of Primary versus Secondary Organic Aerosols from Biomass Burning Plumes over Coastal Ocean Using Sugar Compounds and Stable Carbon Isotopes, *ACS Earth and Space Chemistry*, 3, 1471-1484, 10.1021/acsearthspacechem.9b00140, 2019.
- 380 Bouwman, A. F., Lee, D. S., Asman, W. A. H., Dentener, F. J., VanderHoek, K. W., and Olivier, J. G. J.: A global high-resolution emission inventory for ammonia, *Global Biogeochem Cy*, 11, 561-587, 1997.
- Bray, C. D., Battye, W., Aneja, V. P., Tong, D. Q., Lee, P., and Tang, Y.: Ammonia emissions from biomass burning in the continental United States, *Atmospheric Environment*, 187, 50-61, 385 <https://doi.org/10.1016/j.atmosenv.2018.05.052>, 2018.
- Carmichael, G. R., Ferm, M., Thongboonchoo, N., Woo, J.-H., Chan, L. Y., Murano, K., Viet, P. H., Mossberg, C., Bala, R., Boonjawan, J., Upatum, P., Mohan, M., Adhikary, S. P., Shrestha, A. B., Pienaar, J. J., Brunke, E. B., Chen, T., Jie, T., Guoan, D., Peng, L. C., Dhiharto, S., Harjanto, H., Jose, A. M., Kimani, W., Kirouane, A., Lacaux, J.-P., Richard, S., Barturen, O., Cerda, J. C., Athayde, A., Tavares, 390 T., Cotrina, J. S., and Bilici, E.: Measurements of sulfur dioxide, ozone and ammonia concentrations in Asia, Africa, and South America using passive samplers, *Atmospheric Environment*, 37, 1293-1308, [https://doi.org/10.1016/S1352-2310\(02\)01009-9](https://doi.org/10.1016/S1352-2310(02)01009-9), 2003.
- Chang, Y., Deng, C., Dore, A. J., and Zhuang, G.: Human Excreta as a Stable and Important Source of Atmospheric Ammonia in the Megacity of Shanghai, *Plos One*, 10, e0144661, 2015.
- 395 Chang, Y., Liu, X., Deng, C., Dore, A. J., and Zhuang, G.: Source apportionment of atmospheric ammonia before, during, and after the 2014 APEC summit in Beijing using stable nitrogen isotope signatures, *Atmospheric Chemistry and Physics*, 16, 11635-11647, 10.5194/acp-16-11635-2016, 2016a.
- Chang, Y., and Ma, H.: Comment on "Fossil Fuel Combustion-Related Emissions Dominate Atmospheric Ammonia Sources during Severe Haze Episodes: Evidence from ¹⁵N-Stable Isotope in Size-Resolved Aerosol Ammonium", *Environ Sci Technol*, 50, 10765-10766, 10.1021/acs.est.6b03458, 2016.
- 400 Chang, Y., Zou, Z., Deng, C., Huang, K., Collett, J. L., Lin, J., and Zhuang, G.: The importance of vehicle emissions as a source of atmospheric ammonia in the megacity of Shanghai, *Atmospheric Chemistry and Physics*, 16, 3577-3594, 10.5194/acp-16-3577-2016, 2016b.



- 405 Chang, Y., Zhang, Y. L., Li, J., Tian, C., Song, L., Zhai, X., Zhang, W., Huang, T., Lin, Y. C., Zhu, C.,
Fang, Y., Lehmann, M. F., and Chen, J.: Isotopic constraints on the atmospheric sources and formation
of nitrogenous species in clouds influenced by biomass burning, *Atmos. Chem. Phys.*, 19, 12221-12234,
10.5194/acp-19-12221-2019, 2019a.
- 410 Chang, Y., Zou, Z., Zhang, Y., Deng, C., Hu, J., Shi, Z., Dore, A. J., and Collett, J.: Assessing
contributions of agricultural and non-agricultural emissions to atmospheric ammonia in a Chinese
megacity, *Environmental Science & Technology*, 10.1021/acs.est.8b05984, 2019b.
- Chang, Y., Clarisse, L., Van Damme, M., Tao, Y., Zou, Z., Dore, A. J., and Collett, J. L.: Ammonia
Emissions from Mudflats of River, Lake, and Sea, *ACS Earth and Space Chemistry*,
10.1021/acsearthspacechem.0c00017, 2020.
- 415 Chang, Y. H., Liu, X. J., Dore, A. J., and Li, K.: Stemming PM_{2.5} pollution in China: Re-evaluating the
role of ammonia, aviation and non-exhaust road traffic emissions, *Environmental science & technology*,
46, 13035-13036, 10.1021/es304806k, 2012.
- Chu, J.-E., Kim, K.-M., Lau, W. K. M., and Ha, K.-J.: How Light-Absorbing Properties of Organic
Aerosol Modify the Asian Summer Monsoon Rainfall?, *Journal of Geophysical Research:
Atmospheres*, 123, 2244-2255, 10.1002/2017jd027642, 2018.
- 420 Clarisse, L., Clerbaux, C., Dentener, F., Hurtmans, D., and Coheur, P.-F.: Global ammonia distribution
derived from infrared satellite observations, *Nat Geosci*, 2, 479-483, 10.1038/ngeo551, 2009.
- Clarisse, L., Shephard, M. W., Dentener, F., Hurtmans, D., Cady-Pereira, K., Karagulian, F., Van Damme,
M., Clerbaux, C., and Coheur, P.-F.: Satellite monitoring of ammonia: A case study of the San Joaquin
Valley, *Journal of Geophysical Research: Atmospheres*, 115, 10.1029/2009JD013291, 2010.
- 425 Crutzen, P. J., Heidt, L. E., Krasnec, J. P., Pollock, W. H., and Seiler, W.: Biomass burning as a source
of atmospheric gases CO, H₂, N₂O, NO, CH₃Cl and COS, *Nature*, 282, 253, 10.1038/282253a0, 1979.
- Crutzen, P. J., and Andreae, M. O.: Biomass Burning in the Tropics: Impact on Atmospheric Chemistry
and Biogeochemical Cycles, *Science*, 250, 1669-1678, 10.1126/science.250.4988.1669, 1990.
- 430 Elliott, E. M., Yu, Z., Cole, A. S., and Coughlin, J. G.: Isotopic advances in understanding reactive
nitrogen deposition and atmospheric processing, *Science of The Total Environment*, 662, 393-403,
<https://doi.org/10.1016/j.scitotenv.2018.12.177>, 2019.
- Felix, J. D., Elliott, E. M., Gish, T. J., McConnell, L. L., and Shaw, S. L.: Characterizing the isotopic
composition of atmospheric ammonia emission sources using passive samplers and a combined
oxidation-bacterial denitrifier approach, *Rapid communications in mass spectrometry : RCM*, 27,
435 2239-2246, 10.1002/rcm.6679, 2013.
- Hantson, S., Arneth, A., Harrison, S. P., Kelley, D. I., Prentice, I. C., Rabin, S. S., Archibald, S., Mouillot,
F., Arnold, S. R., Artaxo, P., Bachelet, D., Ciais, P., Forrest, M., Friedlingstein, P., Hickler, T., Kaplan,
J. O., Kloster, S., Knorr, W., Lasslop, G., Li, F., Mangeon, S., Melton, J. R., Meyn, A., Sitch, S., Spessa,
A., van der Werf, G. R., Voulgarakis, A., and Yue, C.: The status and challenge of global fire modelling,
440 *Biogeosciences*, 13, 3359-3375, 10.5194/bg-13-3359-2016, 2016.
- Huang, C., Hu, Q., Lou, S., Tian, J., Wang, R., Xu, C., An, J., Ren, H., Ma, D., Quan, Y., Zhang, Y., and
Li, L.: Ammonia Emission Measurements for Light-Duty Gasoline Vehicles in China and Implications
for Emission Modeling, *Environmental Science & Technology*, 52, 11223-11231,
10.1021/acs.est.8b03984, 2018.



- 445 Huang, K., Fu, J. S., Hsu, N. C., Gao, Y., Dong, X., Tsay, S.-C., and Lam, Y. F.: Impact assessment of biomass burning on air quality in Southeast and East Asia during BASE-ASIA, *Atmospheric Environment*, 78, 291-302, <https://doi.org/10.1016/j.atmosenv.2012.03.048>, 2013.
- Kawashima, H., and Kurahashi, T.: Inorganic ion and nitrogen isotopic compositions of atmospheric aerosols at Yurihonjo, Japan: Implications for nitrogen sources, *Atmospheric environment*, 45, 6309-6316, 2011.
- 450 Layman, C. A., Araujo, M. S., Boucek, R., Hammerschlag-Peyer, C. M., Harrison, E., Jud, Z. R., Matich, P., Rosenblatt, A. E., Vaudo, J. J., Yeager, L. A., Post, D. M., and Bearhop, S.: Applying stable isotopes to examine food-web structure: an overview of analytical tools, *Biological Reviews*, 87, 545-562, [10.1111/j.1469-185X.2011.00208.x](https://doi.org/10.1111/j.1469-185X.2011.00208.x), 2012.
- 455 Lee, H. H., Bar-Or, R. Z., and Wang, C.: Biomass burning aerosols and the low-visibility events in Southeast Asia, *Atmos. Chem. Phys.*, 17, 965-980, [10.5194/acp-17-965-2017](https://doi.org/10.5194/acp-17-965-2017), 2017.
- Li, F., Zhang, X., and Kondragunta, S.: Biomass Burning in Africa: An Investigation of Fire Radiative Power Missed by MODIS Using the 375 m VIIRS Active Fire Product, *Remote Sensing*, 12, [10.3390/rs12101561](https://doi.org/10.3390/rs12101561), 2020.
- 460 Li, Q., Jiang, J., Cai, S., Zhou, W., Wang, S., Duan, L., and Hao, J.: Gaseous Ammonia Emissions from Coal and Biomass Combustion in Household Stoves with Different Combustion Efficiencies, *Environmental Science & Technology Letters*, 3, 98-103, [10.1021/acs.estlett.6b00013](https://doi.org/10.1021/acs.estlett.6b00013), 2016.
- Liu, D., Fang, Y., Tu, Y., and Pan, Y.: Chemical method for nitrogen isotopic analysis of ammonium at natural abundance, *Anal Chem*, 86, 3787-3792, [10.1021/ac403756u](https://doi.org/10.1021/ac403756u), 2014.
- 465 Liu, X., Zhang, Y., Han, W., Tang, A., Shen, J., Cui, Z., Vitousek, P., Erisman, J. W., Goulding, K., Christie, P., Fangmeier, A., and Zhang, F.: Enhanced nitrogen deposition over China, *Nature*, 494, 459-462, [10.1038/nature11917](https://doi.org/10.1038/nature11917), 2013.
- Lobert, J. M., Scharffe, D. H., Hao, W. M., and Crutzen, P. J.: Importance of biomass burning in the atmospheric budgets of nitrogen-containing gases, *Nature*, 346, 552-554, [10.1038/346552a0](https://doi.org/10.1038/346552a0), 1990.
- 470 Marlier, M. E., DeFries, R. S., Voulgarakis, A., Kinney, P. L., Randerson, J. T., Shindell, D. T., Chen, Y., and Faluvegi, G.: El Niño and health risks from landscape fire emissions in southeast Asia, *Nat Clim Chang*, 3, 131-136, [10.1038/nclimate1658](https://doi.org/10.1038/nclimate1658), 2013.
- Martin, R. V.: Satellite remote sensing of surface air quality, *Atmospheric Environment*, 42, 7823-7843, <https://doi.org/10.1016/j.atmosenv.2008.07.018>, 2008.
- 475 Pan, X., Ichoku, C., Chin, M., Bian, H., Darmenov, A., Colarco, P., Ellison, L., Kucsera, T., da Silva, A., Wang, J., Oda, T., and Cui, G.: Six Global Biomass Burning Emission Datasets: Inter-comparison and Application in one Global Aerosol Model, *Atmos. Chem. Phys. Discuss.*, 2019, 1-39, [10.5194/acp-2019-475](https://doi.org/10.5194/acp-2019-475), 2019.
- Parnell, A. C., Inger, R., Bearhop, S., and Jackson, A. L.: Source partitioning using stable isotopes: coping with too much variation, *Plos One*, 5, e9672, 2010.
- 480 Paulot, F., and Jacob, D. J.: Hidden cost of US agricultural exports: particulate matter from ammonia emissions, *Environmental science & technology*, 48, 903-908, 2014.
- Paulot, F., Paynter, D., Ginoux, P., Naik, V., Whitburn, S., Van Damme, M., Clarisse, L., Coheur, P.-F., and Horowitz, L. W.: Gas-aerosol partitioning of ammonia in biomass burning plumes: Implications for the interpretation of spaceborne observations of ammonia and the radiative forcing of ammonium nitrate, *Geophysical Research Letters*, 44, 8084-8093, [10.1002/2017gl074215](https://doi.org/10.1002/2017gl074215), 2017.



- Puchalski, M. A., Sather, M. E., Walker, J. T., Lehmann, C. M., Gay, D. A., Mathew, J., and Robarge, W. P.: Passive ammonia monitoring in the United States: Comparing three different sampling devices, *Journal of Environmental Monitoring*, 13, 3156-3167, 2011.
- 490 Shi, Y., Matsunaga, T., and Yamaguchi, Y.: High-Resolution Mapping of Biomass Burning Emissions in Three Tropical Regions, *Environmental Science & Technology*, 49, 10806-10814, 10.1021/acs.est.5b01598, 2015.
- Souri, A. H., Choi, Y., Jeon, W., Kochanski, A. K., Diao, L., Mandel, J., Bhawe, P. V., and Pan, S.: Quantifying the Impact of Biomass Burning Emissions on Major Inorganic Aerosols and Their
495 Precursors in the U.S, *Journal of Geophysical Research: Atmospheres*, 122, 12,020-012,041, 10.1002/2017jd026788, 2017.
- Streets, D. G., Canty, T., Carmichael, G. R., de Foy, B., Dickerson, R. R., Duncan, B. N., Edwards, D. P., Haynes, J. A., Henze, D. K., Houyoux, M. R., Jacob, D. J., Krotkov, N. A., Lamsal, L. N., Liu, Y., Lu, Z., Martin, R. V., Pfister, G. G., Pinder, R. W., Salawitch, R. J., and Wecht, K. J.: Emissions estimation
500 from satellite retrievals: A review of current capability, *Atmospheric Environment*, 77, 1011-1042, <https://doi.org/10.1016/j.atmosenv.2013.05.051>, 2013.
- Sun, K., Tao, L., Miller, D. J., Pan, D., Golston, L. M., Zondlo, M. A., Griffin, R. J., Wallace, H. W., Leong, Y. J., Yang, M. M., Zhang, Y., Mauzerall, D. L., and Zhu, T.: Vehicle Emissions as an Important Urban Ammonia Source in the United States and China, *Environmental Science & Technology*, 51,
505 2472-2481, 10.1021/acs.est.6b02805, 2017.
- Sutton, M. A., Erisman, J. W., Dentener, F., and Moller, D.: Ammonia in the environment: From ancient times to the present, *Environmental Pollution*, 156, 583-604, DOI 10.1016/j.envpol.2008.03.013, 2008.
- Sutton, M. A., Oenema, O., Erisman, J. W., Leip, A., van Grinsven, H., and Winiwarter, W.: Too much of a good thing, *Nature*, 472, 159-161, Doi 10.1038/472159a, 2011.
- 510 Tang, Y. S., Braban, C. F., Dragosits, U., Dore, A. J., Simmons, I., van Dijk, N., Poskitt, J., Dos Santos Pereira, G., Keenan, P. O., Conolly, C., Vincent, K., Smith, R. I., Heal, M. R., and Sutton, M. A.: Drivers for spatial, temporal and long-term trends in atmospheric ammonia and ammonium in the UK, *Atmos. Chem. Phys.*, 18, 705-733, 10.5194/acp-18-705-2018, 2018.
- Teng, X., Hu, Q., Zhang, L., Qi, J., Shi, J., Xie, H., Gao, H., and Yao, X.: Identification of Major Sources
515 of Atmospheric NH₃ in an Urban Environment in Northern China During Wintertime, *Environmental Science & Technology*, 51, 6839-6848, 10.1021/acs.est.7b00328, 2017.
- Tsai, Y. I., Sopajaree, K., Chotruksa, A., Wu, H.-C., and Kuo, S.-C.: Source indicators of biomass burning associated with inorganic salts and carboxylates in dry season ambient aerosol in Chiang Mai Basin, Thailand, *Atmospheric Environment*, 78, 93-104, <https://doi.org/10.1016/j.atmosenv.2012.09.040>,
520 2013.
- Van Damme, M., Clarisse, L., Heald, C. L., Hurtmans, D., Ngadi, Y., Clerbaux, C., Dolman, A. J., Erisman, J. W., and Coheur, P. F.: Global distributions, time series and error characterization of atmospheric ammonia (NH₃) from IASI satellite observations, *Atmos. Chem. Phys.*, 14, 2905-2922, 10.5194/acp-14-2905-2014, 2014.
- 525 Van Damme, M., Clarisse, L., Dammers, E., Liu, X., Nowak, J. B., Clerbaux, C., Flechard, C. R., Galy-Lacaux, C., Xu, W., Neuman, J. A., Tang, Y. S., Sutton, M. A., Erisman, J. W., and Coheur, P. F.: Towards validation of ammonia (NH₃) measurements from the IASI satellite, *Atmos. Meas. Tech.*, 8, 1575-1591, 10.5194/amt-8-1575-2015, 2015a.



- 530 Van Damme, M., Erismann, J. W., Clarisse, L., Dammers, E., Whitburn, S., Clerbaux, C., Dolman, A. J.,
and Coheur, P.-F.: Worldwide spatiotemporal atmospheric ammonia (NH₃) columns variability
revealed by satellite, *Geophysical Research Letters*, 42, 8660-8668, 10.1002/2015gl065496, 2015b.
- Van Damme, M., Whitburn, S., Clarisse, L., Clerbaux, C., Hurtmans, D., and Coheur, P. F.: Version 2 of
the IASI NH₃ neural network retrieval algorithm: near-real-time and reanalysed datasets, *Atmos. Meas.
Tech.*, 10, 4905-4914, 10.5194/amt-10-4905-2017, 2017.
- 535 Van Damme, M., Clarisse, L., Whitburn, S., Hadji-Lazaro, J., Hurtmans, D., Clerbaux, C., and Coheur,
P.-F.: Industrial and agricultural ammonia point sources exposed, *Nature*, 564, 99-103,
10.1038/s41586-018-0747-1, 2018.
- van der Werf, G. R., Randerson, J. T., Giglio, L., Collatz, G. J., Kasibhatla, P. S., and Arellano Jr, A. F.:
Interannual variability in global biomass burning emissions from 1997 to 2004, *Atmos. Chem. Phys.*,
540 6, 3423-3441, 10.5194/acp-6-3423-2006, 2006.
- Wang, S. X., Xing, J., Jang, C. R., Zhu, Y., Fu, J. S., and Hao, J. M.: Impact Assessment of Ammonia
Emissions on Inorganic Aerosols in East China Using Response Surface Modeling Technique,
Environmental Science & Technology, 45, 9293-9300, 2011.
- Wang, Y., Zhang, Q. Q., He, K., Zhang, Q., and Chai, L.: Sulfate-nitrate-ammonium aerosols over China:
545 response to 2000–2015 emission changes of sulfur dioxide, nitrogen oxides, and ammonia,
Atmospheric Chemistry and Physics, 13, 2635-2652, 10.5194/acp-13-2635-2013, 2013.
- Whitburn, S., Van Damme, M., Kaiser, J. W., van der Werf, G. R., Turquety, S., Hurtmans, D., Clarisse,
L., Clerbaux, C., and Coheur, P. F.: Ammonia emissions in tropical biomass burning regions:
Comparison between satellite-derived emissions and bottom-up fire inventories, *Atmospheric
Environment*, 121, 42-54, <https://doi.org/10.1016/j.atmosenv.2015.03.015>, 2015.
- 550 Whitburn, S., Van Damme, M., Clarisse, L., Bauduin, S., Heald, C. L., Hadji-Lazaro, J., Hurtmans, D.,
Zondlo, M. A., Clerbaux, C., and Coheur, P. F.: A flexible and robust neural network IASI-NH₃
retrieval algorithm, *Journal of Geophysical Research: Atmospheres*, 121, 6581-6599,
10.1002/2016JD024828, 2016a.
- 555 Whitburn, S., Van Damme, M., Clarisse, L., Turquety, S., Clerbaux, C., and Coheur, P.-F.: Doubling of
annual ammonia emissions from the peat fires in Indonesia during the 2015 El Niño, *Geophysical
Research Letters*, 43, 11,007-011,014, 10.1002/2016gl070620, 2016b.
- Zheng, X.-D., Liu, X.-Y., Song, W., Sun, X.-C., and Liu, C.-Q.: Nitrogen isotope variations of ammonium
across rain events: Implications for different scavenging between ammonia and particulate ammonium,
560 *Environmental Pollution*, 239, 392-398, <https://doi.org/10.1016/j.envpol.2018.04.015>, 2018.
- Zhu, L., Henze, D. K., Cady-Pereira, K. E., Shephard, M. W., Luo, M., Pinder, R. W., Bash, J. O., and
Jeong, G.-R.: Constraining U.S. ammonia emissions using TES remote sensing observations and the
GEOS-Chem adjoint model, *Journal of Geophysical Research: Atmospheres*, 118, 3355-3368,
10.1002/jgrd.50166, 2013.
- 565